Outage Performance Analysis in Cognitive RIS-NOMA System under Imperfect CSI

K. Xue[1], M. Li[1*], W. Chen[2], Z. Han[3, 4] and H. Yuan[5]

[1] School of Electronics Information Engineering, Taiyuan University of Science and Technology, China.
Email:s202115110169@stu.tyust.edu.cn and meilingli@tyust.edu.cn[*]

[2] Beijing National Research Center for Information Science and Technology,
Department of Electronic Engineering Tsinghua University, Beijing, China.
Email:wchen@tsinghua.edu.cn

[3] Department of Electrical and Computer Engineering University of Houston, USA.

[4] Department of Computer Science and Engineering Kyung Hee University, South Korean.
Email:hanzhu22@gmail.com

[5] School of Computer Science and Mathematics, Kingston University, KT1 2EE, UK.
Email: H.Yuan@kingston.ac.uk

Abstract—**Cognitive non-orthogonal multiple access (NOMA) and reconfigurable intelligent surface (RIS) have been envisioned as two promising technologies for vehicle to everything (V2X) networks. This paper considers an RIS-aided V2X network with cognitive NOMA while considering the imperfect channel state information (CSI) due to the mobility of the vehicles. The new approximate outage probability (OP) expressions of the supposed system are derived over double Rayleigh fading channels. Numerical and Monte Carlo simulation results are presented to corroborate the analysis. The results demonstrated that imperfect CSI has a significant but different impact on the outage performance of the far and near users, which are also different under different numbers of reflecting units.**

Index Terms—**Vehicle to everything, intelligent reflecting surface, cognitive non-orthogonal multiple access, outage performance, channel estimation errors**

I. INTRODUCTION

With the upcoming sixth generation (6G) of wireless systems, vehicular communications will be an instrumental element of future connected autonomous vehicles. However, the fast growth of the number of connected vehicles in vehicular networks results in challenges associated with the quality of vehicular communications, such as low access efficiency, spectrum scarcity and severe data congestion [1]. Therefore, it is necessary to effectively improve and deal with these challenges to ensure the safe and reliable transmission of data [2].

To improve the spectrum efficiency and reduce signalling cost and resource collisions, cognitive radio (CR) technology can sense the available frequency resource intelligently by dynamic spectrum access and sharing, which is suitable for the heterogeneous dynamic communication scenarios in vehicular communications [3] [4].

In addition, non-orthogonal multiple access (NOMA) with high spectrum efficiency and supporting giant connections has been viewed as a promising multiple access candidate for 6G networks. It has been shown that more efficient spectrum utilization can be achieved by combining CR and NOMA, by which the requirement of lower latency and massive connectivity can be better satisfied [5]. Further,

reconfigurable intelligent surface (RIS) can enhance vehicular channel conditions by introducing enhanced multi-path propagation and achieving larger transmission coverage [6].

In the existing related literature, the authors in [7] studied the outage probability (OP) of an underlay based CR-NOMA network considering the imperfect CSI. In [8], the authors studied the OP and bit error rate (BER) of an underlay based CR-NOMA vehicle communications. The authors in [9] studied the OP performance of a CR-NOMA network based on incremental relay. The authors in [10] investigated the RIS-aided NOMA network under hardware impairment.

While the literature has laid a basic foundation for understanding the applications of RIS aided NOMA, the outage performance of the cognitive NOMA-RIS based vehicle to everything (V2X) network for a unified framework still needs to be investigated. Different from previous works, we proposed a novel cognitive NOMA-RIS aided V2X network and derived the approximate closed-form expressions of OP for the cognitive users subject to the Double-Rayleigh fading while taking into account the imperfect CSI and the interference from the primary user. The numerical and analysis results show that the RIS-NOMA strategy can achieve lower OP in the considered interweave based Cognitive NOMA-RIS aided V2X network. Also, the channel estimation error (CEE) affects the outage performance of both near and far users.

II. SYSTEM MODEL

As depicted in Fig. 1, we propose a downlink RIS aided V2X network with cognitive NOMA transmission in the secondary links. The secondary network includes a source vehicle V_s and multiple destination vehicles (DVs) for data transmission opportunistically by implementing a spectrum sensing (SS) scheme, whereas V_s equipped with RIS as the access point and transmits data to DVs in the surroundings of V_s in the power domain NOMA mode. According to the SS policy, the DVs can utilize the spectrum exclusively when vacant. Let $\mathcal{H}_0$ and $\mathcal{H}_1$ denote the event that the
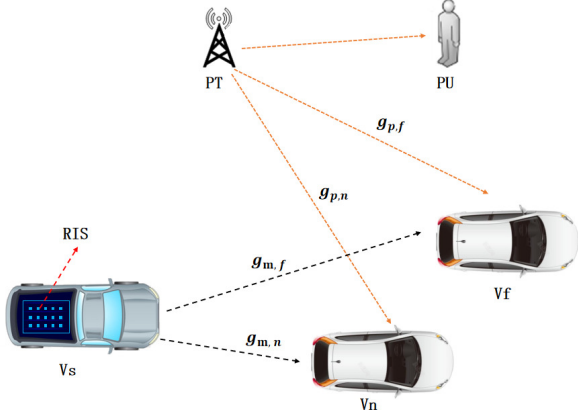
Fig. 1. RIS aided V2X network with cognitive NOMA transmission.

licensed spectrum is either unoccupied or occupied by the primary users (PUs) during a time slot, respectively, whereas $\mathcal{H}$ and $\hat{\mathcal{H}}$ account for the real status of PU's spectrum and its counterpart detected by DVs, respectively. Due to the background noise and fading effects, achieving a perfectly reliable SS is impossible. Consequently, if the missed detection happens, the presence of PU causes interference to DVs and vice versa. Let η be the interference level of the PU on DVs, i.e., $\eta = 0$ when $\hat{\mathcal{H}} = \mathcal{H}_0$ with $\mathcal{H} = \mathcal{H}_0$ and $\eta \neq 0$ if $\hat{\mathcal{H}} = \mathcal{H}_0$ with $\mathcal{H} = \mathcal{H}_1$, corresponding to either unoccupied or occupied licensed spectrum, respectively. Thereafter, the probability of successful detection of PU P_d and the false alarm probability P_f are defined as $P_d = \Pr\left(\hat{\mathcal{H}} = \mathcal{H}_1 | \mathcal{H} = \mathcal{H}_1\right)$ and $P_f = \Pr\left(\hat{\mathcal{H}} = \mathcal{H}_1 | \mathcal{H} = \mathcal{H}_0\right)$ [11].

As depicted in Fig. 1, we assume that V_s reflected the superimposed symbols $x_s = \sqrt{\alpha_n P_s}x_n + \sqrt{\alpha_f P_s}x_f$ to DVs via RIS, where P_s is the total transmitted signal power, while x_n and x_f are the transmission signals for V_n and V_f with $E\left[|x_n|^2\right] = E\left[|x_f|^2\right] = 1$. The corresponding power allocation coefficients α_n and α_f satisfy the relationship $\alpha_n < \alpha_f$ and $\alpha_n + \alpha_f = 1$. Without loss of generality, we also assume that RIS know the channel phase information, which has the ability to adjust the RIS phase by phase cancellation and proper alignment of reflected signals from RIS to maximize the signal-to-interference-plus-noise ratio (SINR) of received signals [12]. Referring to channel estimation error mode using linear minimum mean square error (MMSE) in [13], the received signal of $V_i, i \in \{n, f\}$ can be expressed as

$$y_i = (\hat{g}_{p,i} + e_{p,i})\sqrt{\eta P_T d_{p,i}^{-\beta}}x_p + n_i + \sum_{m=1}^{M}(\hat{g}_{m,i} + e_{m,i})$$
$$\times |r_m|e^{-j\theta_m}\sqrt{d_{m,i}^{-\beta}P_S}\left(\sqrt{\alpha_n}x_n + \sqrt{\alpha_f}x_f\right),$$
(1)

where x_p and P_T are the transmit signal of the PT and the corresponding transmission power, $\hat{g}_{p,i}$ and $\hat{g}_{m,i}$ are the estimated channel coefficients between the links from the PT and the m-th reflection element of the RIS to V_i respectively, M is the number of RIS reflection units, $e_{p,i}$ and $e_{m,i}$ are the corresponding channel estimation errors which can be

modeled as complex Gaussian random variable (CGRV) with $e_{p,i} \sim CN\left(0, \sigma_{e_{p,i}}^2\right)$ and $e_{m,i} \sim CN\left(0, \sigma_{e_{m,i}}^2\right)$, $\sigma_{e_{m,i}}^2$ represents the error level of the channel estimation error, $d_{p,i}^{-\beta}$ and $d_{m,i}^{-\beta}$ are the path loss during the links from the PT and the m-th reflection element of the RIS to V_i, respectively, with path loss exponent β, $d_{p,i}$ and $d_{m,i}$ are the distances from the PT and the m-th reflection element of the RIS to V_i, $|r_m|$ denotes the reflection gain of the m-th reflection element of the RIS with $|r_m| = 1$ for maximizing the received SINR, n_i is the additive white Gaussian noise (AWGN) with mean power N_0 at V_i.

According to the principle of power domain NOMA, each user decodes and cancels out weaker users' signals before decoding its message with successive interference cancellation (SIC) technology. By weaker users, we refer to the users with lower link gains than the considered user, and more powerful resources are allocated to such users. SIC is carried out to detect and subtract the signals of all other weaker users. Precisely, the weaker user V_f will decode its signal x_f by treating the stronger user signal x_n as an additional noise. While the stronger user V_n will first detect and subtract the signal x_f and then decode it's signal x_n without any interference. Then, the instantaneous SINR for decoding x_f at V_i can be evaluated as (2) at the top of the next page, where $A_i = \sum_{m=1}^{M}|\hat{g}_{m,i}|$ and $E_i = \sum_{m=1}^{M}\sigma_{e_{m,i}}^2$. Particularly, the strongest user V_n will not suffer from interference by other users after the earlier detection step. Then, the achievable SINR for V_n detecting its signal can be written as

$$\gamma_n^{x_n} = \frac{\alpha_n P_S A_n^2 d_n^{-\beta}}{\eta P_T\left(|\hat{g}_{p,n}|^2 + \sigma_{e_{p,n}}^2\right)d_{p,n}^{-\beta} + E_n P_S d_n^{-\beta} + N_0}.$$
(3)

III. OUTAGE PERFORMANCE

A. The Outage Probability of V_f

In the following, we consider that the connection between V_s and DVs can be established. V_s send information to DVs at a constant rate of R_i for legitimate user V_i. The OP is calculated when the primary users detect the licensed spectrum unoccupied. Let Δ_μ denote the probability that the current status of the primary user's spectrum is $\mathcal{H}_\mu$ given that DVs detected it to be unoccupied, i.e., $\Delta_\mu = \Pr\left(\mathcal{H} = \mathcal{H}_\mu | \hat{\mathcal{H}} = \mathcal{H}_0\right)$, with $\mu = \{0, 1\}$. As described in Section II, V_f decode its signal x_f by treating x_n as interference. When the instantaneous SINR of V_f is smaller than the target γ_f, with $\gamma_f = 2^{R_f} - 1$, the outage happens for V_f, i.e., the OP of the considered system for V_f can be expressed as

$$P_{out,f} = \Pr\left(\gamma_f^{x_f} < \gamma_f | \hat{\mathcal{H}} = \mathcal{H}_0\right)$$
$$= \sum_{\mu=0}^{1}\Delta_\mu \underbrace{\Pr\left(\gamma_f^{x_f} < \gamma_f | \mathcal{H} = \mathcal{H}_\mu, \hat{\mathcal{H}} = \mathcal{H}_0\right)}_{P_{o,f}^\mu},$$
(4)

$$\gamma_i^{x_f} = \frac{\alpha_f P_S A_i^2 d_i^{-\beta}}{\eta P_T \left(|\hat{g}_{p,i}|^2 + \sigma_{e_{p,i}}^2\right) d_{p,i}^{-\beta} + (\alpha_n A_i^2 + E_i) P_S d_i^{-\beta} + N_0}. \tag{2}$$

Let $P_0 = \Pr(\mathcal{H} = \mathcal{H}_0)$ be the probability that the authorized spectrum is unoccupied by the PU. According to the Bayes criterion, one can check that

$$\Delta_\mu = \frac{\Pr\left(\hat{\mathcal{H}}|\mathcal{H} = \mathcal{H}_\mu\right) \Pr\left(\mathcal{H} = \mathcal{H}_\mu\right)}{\sum_{\delta=0}^{1} \Pr\left(\hat{\mathcal{H}} = \mathcal{H}_0|\mathcal{H} = \mathcal{H}_\delta\right) \Pr\left(\mathcal{H} = \mathcal{H}_\delta\right)}$$
$$= \begin{cases} \frac{P_0(1-P_f)}{P_0(1-P_f)+(1-P_0)(1-P_d)}, \mu = 0, \\ \frac{(1-P_0)(1-P_d)}{P_0(1-P_f)+(1-P_0)(1-P_d)}, \mu = 1. \end{cases} \tag{5}$$

As it can be seen that it is complex to obtain the closed results of (4), we introduce Theorem 1 to show the closed expressions, and the detailed proof can be found in the Appendix thereafter.

Theorem 1: The OP expressions of the considered system for weaker user V_f can be written as

$$P_{out,f} = \begin{cases} \Delta_0 + \Delta_1, \alpha_f \leq T_1, \\ \Delta_0 P_{o,f}^0 + \Delta_1 P_{o,f}^1, \alpha_f > T_1, \end{cases} \tag{6}$$

where $T_1 = \frac{\gamma_f}{1+\gamma_f}$, $P_{o,f}^1$ can be obtained by replacing i by f in (7) shown on the top of the next page, $D_p(z) = 2^{\frac{p}{2}} e^{-\frac{z^2}{4}} \left\{ \frac{\sqrt{\pi}}{\Gamma(\frac{1-p}{2})} \Phi\left(-\frac{p}{2}, \frac{1}{2}; \frac{z^2}{2}\right) - \frac{\sqrt{2\pi}z}{\Gamma(-\frac{p}{2})} \Phi\left(\frac{1-p}{2}, \frac{3}{2}; \frac{z^2}{2}\right) \right\}$ is Parabolic Cylinder function, $\Phi(\alpha, \gamma; z) = \sum_{q=0}^{Q} \frac{(\alpha+q-1)!/(\alpha-1)!}{(\gamma+q-1)!/(\gamma-1)!} \frac{z^q}{q!}$, $\phi_l = \cos\left(\frac{2l-1}{2L}\pi\right)$, L is the parameter to ensure the complexity-accuracy trade-off, and

$$P_{o,f}^0 = \frac{\gamma\left(a+1, \frac{1}{b}\sqrt{\frac{\psi_{1,f}}{P_S}}\right)}{\Gamma(a+1)}, \tag{8}$$

$$\psi_{1,i} = \frac{\gamma_f \left(P_S E_i + d_i^\beta N_0\right)}{(\alpha_f - \alpha_n \gamma_f)}, \tag{9}$$

$$\varepsilon_i = \frac{(\alpha_f - \alpha_n \gamma_f) d_{p,i}^\beta}{\eta P_T d_i^\beta \gamma_f}, \tag{10}$$

$$\tau_i = \frac{\eta P_T d_i^\beta \sigma_{e_{p,i}}^2 + P_S d_{p,i}^\beta E_i + d_{p,i}^\beta d_i^\beta N_0}{\eta P_T d_i^\beta}. \tag{11}$$

Proof. See Appendix A.

B. The Outage Probability of V_n

For the stronger user, the SIC is carried out first to detect and subtract the weaker user's signal and then decode it. To this end, the outage event happens for the stronger user V_n in the following two circumstances: (i) V_n cannot subtract and decode the signal x_f correctly; (ii) V_n can decode x_f successfully by SIC, while it cannot decode its own signal

x_n successfully. Therefore, the OP of V_n can be evaluated by

$$P_{out,n} = 1 - \Pr\left(\gamma_n^{x_f} > \gamma_f, \gamma_n^{x_n} > \gamma_n | \hat{\mathcal{H}} = \mathcal{H}_0\right)$$
$$= 1 -$$
$$\sum_{\mu=0}^{1} \Delta_\mu \underbrace{\Pr\left(\gamma_n^{x_f} > \gamma_f, \gamma_n^{x_n} > \gamma_n | \mathcal{H} = \mathcal{H}_\mu, \hat{\mathcal{H}} = \mathcal{H}_0\right)}_{P_{o,n}^\mu}, \tag{12}$$

where $\gamma_n = 2^{R_n} - 1$ is the target SINR for V_n decoding signal x_n, the OP of user V_n with imperfect CSI can be provided in the following theorem.

As it can be seen that it is complex to obtain the closed results of (12), we introduce Theorem 2 to show the closed expressions and the detailed proof can be found in the Appendix thereafter.

Theorem 2: The OP expressions of the considered system for strong user V_n can be written as

$$P_{out,n} = \begin{cases} 1, \alpha_f \leq T_1, \\ 1 - \Delta_0 P_{o,n}^0 - \Delta_1\left(1 - P_{o,n}^1\right), T_1 < \alpha_f \leq T_2, \\ 1 - \Delta_0 P_{o,n}^0 - \Delta_1\left(1 - F_{o,n}\right), T_2 < \alpha_f < 1, \end{cases} \tag{13}$$

with $T_2 = 1 - \frac{\gamma_n}{\gamma_f + \gamma_n + \gamma_f \gamma_n}$, $P_{o,n}^1$ can be obtained by replacing i by n in (8), $F_{o,n}$ corresponds to $P_{o,n}^1$ when $\varepsilon_n = \varepsilon_{2,n}$ in (8), and

$$P_{o,n}^0 = 1 - \frac{\gamma\left(a+1, \frac{1}{b}\sqrt{\frac{\psi_n^*}{P_S}}\right)}{\Gamma(a+1)}, \tag{14}$$

$$\varepsilon_{2,n} = \frac{\alpha_n d_{p,n}^\beta}{\eta P_T d_n^\beta \gamma_n}, \tag{15}$$

where $\psi_n^* = \max(\psi_{1,n}, \psi_{2,n})$, $\psi_{1,n}$ can be obtained by replacing i by n in (9), $\psi_{2,n} = \frac{\gamma_n\left(E_n P_S + N_0 d_n^\beta\right)}{\alpha_n}$.

Proof. See Appendix B.

IV. SIMULATION RESULTS

In this section, the secure transmission performance in terms of outage probabilities of the considered RIS-NOMA assisted cognitive V2X networks is presented by numerical and Monte Carlo simulations to validate the derived analytical results when the imperfect CSI exists. Without otherwise stated, the simulation parameters are defined as follows. The transmit power P_s is 40dB. The path loss exponent is $\beta = 2.7$. The power allocation coefficients are $\alpha_n = 0.2$ and $\alpha_f = 0.8$. The target rate are set to $R_n = 2$bps/Hz and $R_f = 1$bps/Hz. The interference level is $\eta = 0.6$. The distance between V_s and V_i are set $d_{m,n} = 5$m and $d_{m,f} = 10$m. The distance between P_T and V_i are set $d_{p,n} = 20$m and $d_{p,f} = 30$m. The number of RIS's RUs is set to $N = 10$.

$$P_{o,i}^1 = \frac{\gamma\left(a+1,\frac{1}{b}\sqrt{\frac{\tau_i}{\varepsilon_i P_S}}\right)}{\Gamma(a+1)} + \frac{1}{b^{a+1}}\exp\left(\frac{\tau_i}{\lambda_{p,i}}\right)\left(\frac{2\varepsilon_i P_S}{\lambda_{p,i}}\right)^{-\frac{a+1}{2}}\exp\left(\frac{\lambda_{p,i}}{8b^2\varepsilon_i P_S}\right)D_{-(a+1)}\left(\frac{1}{b}\sqrt{\frac{\lambda_{p,i}}{2\varepsilon_i P_S}}\right)$$
$$-\exp\left(\frac{\tau_i}{\lambda_{p,i}}\right)\frac{\pi}{L}\sum_{l=1}^{L}\frac{\sqrt{1-\phi_l^2}(\phi_l+1)^{\frac{a-1}{2}}}{2b^{a+1}\Gamma(a+1)}\left(\frac{\tau_i}{2\varepsilon_i P_S}\right)^{\frac{a+1}{2}}\exp\left(-\frac{\tau_i(\phi_l+1)}{2\lambda_{p,i}}-\frac{1}{b}\sqrt{\frac{\tau_i(\phi_l+1)}{2\varepsilon_i P_S}}\right). \tag{7}$$

The OP performance for the far user and the near user with different reflecting numbers of RIS has been illustrated in Figs. 2. The exact analytical curves of OP for user V_i are plotted based on (6) and (14). It can be seen that the derived analysis is corroborated with the simulation results, where it is shown that the derived analysis and simulation results match perfectly for both users over the entire transmit power range. One can be observed that OP decreases monotonously with the increase of P_s for a fixed reflecting number of RIS N under imperfect CSI case. Moreover, the valuable founding is that the OP performance of the near user V_n will not always be necessarily better than that of far user V_f due to the impact of imperfect CSI, which shows that the power allocation needs to be reconsidered in order to serve the near user more better in the actual scenarios.
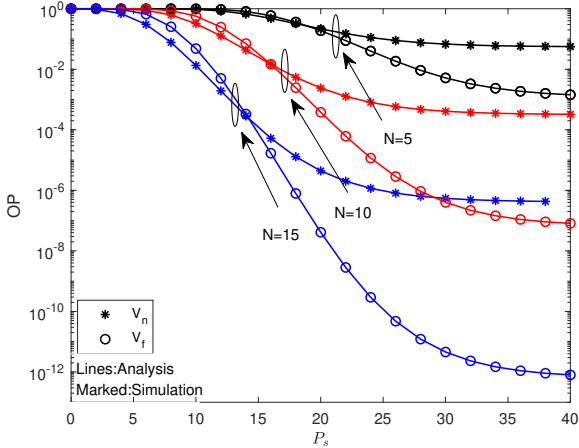

Fig. 2. OP vs transmitting power of V_s under imperfect CSI case with different number of N

Fig. 3 shows the influence of different levels of σ_e^2 on OP performance. Such CSI term impacts the outage of V_n and V_f. It can be seen that with the increasing of σ_e^2, the outage performance of V_i becomes worse, which is due to the smaller σ_e^2 leading to a smaller performance gap among two vehicles. Moreover, we can observed that with the increase of P_s level, the influence of σ_e^2 on OP gradually increases. Which indicates that limiting CSI imperfections under high transmitting power area makes maintaining outage performance at a reasonable value possible.

V. CONCLUSION

This paper establishes a system model of the RIS-aided V2X network with cognitive NOMA. The outage performance of the system is studied and analyzed from the perspective of reliability in terms of OP under the assumption of the double Rayleigh fading channel. In order to
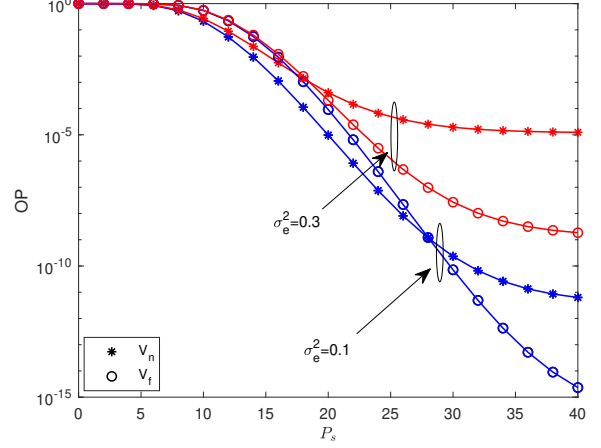

Fig. 3. OP vs transmitting power of V_s under imperfect CSI case with different σ_e^2

consider the actual factors, the CEE affects is introduced to evaluate the impact of imperfect CSI, and the new analytical expressions of the OP have been derived. The simulation results show that the outage performance of the considered network can be improved in terms of transmitting power of source vehicles, levels of CEE affects and the number of RIS reflection units. These findings further promote the applicability of cognitive NOMA networks and RIS techniques in V2X networks.

APPENDIX A: PROOF OF THEOREM 1

In order to obtain the closed-form of (4), we should firstly get the results of $P_{o,f}^0$ and $P_{o,f}^1$ with $\mu = 0$ and $\mu = 1$ in (4). Let $i = f$ in (2) and substitute it into $P_{o,f}^0$ in (4), we arrive at

$$P_{o,f}^0 = \Pr\left(\frac{\alpha_f P_S A_f^2 d_f^{-\beta}}{\left(\alpha_n A_f^2 + E_f\right)P_S d_f^{-\beta} + N_0} < \gamma_f\right)$$
$$= \Pr\left(A_f^2\left(\alpha_f - \alpha_n\gamma_f\right) < \frac{\gamma_f\left(P_S E_f + d_f^\beta N_0\right)}{P_S}\right). \tag{A.1}$$

Let $Y = A_i^2$, according to [14], the PDF and CDF of Y can be tightly approximated as the first term of a Laguerre series expansion as shown bellows

$$f_Y(y) = \frac{y^{\frac{a-1}{2}}}{2b^{a+1}\Gamma(a+1)}\exp\left(-\frac{\sqrt{y}}{b}\right), \tag{A.2}$$

$$F_Y(y) = \frac{\gamma\left(a+1,\frac{\sqrt{y}}{b}\right)}{\Gamma(a+1)}, \tag{A.3}$$

where $\alpha_i = \frac{k_1^2}{k_2} - 1$, $b_i = \frac{k_2}{k_1}$, $k_1 = \frac{\lambda_m^2 M \pi}{2}$, $k_2 = 4M\lambda_m^4 \left(1 - \frac{\pi^2}{16}\right)$, λ_m denote the parameter that measures the quality of the channel between the m-th reflection element of RIS and V_i when it is Rayleigh channel.

When $\alpha_f \leq T_1$, we can easily obtain $P_{o,f}^0 = 1$; When $\alpha_f > T_1$, we arrive at

$$P_{o,f}^0 = \Pr\left(A_f^2 < \frac{\psi_{1,f}}{P_S}\right), \qquad (A.4)$$

Using (A.3) into (A.4), we can obtain the results of (8).

In another side, substituting (2) and letting $i = f$ into $P_{o,f}^1$ in (4), $P_{o,f}^1$ can be given by (A.5) at the top of the next page.

Let $\tau_f = \frac{\eta P_T d_f^\beta \sigma_{e_{p,f}}^2 + P_S d_{p,f}^\beta E_f + d_{p,f}^\beta d_f^\beta N_0}{\eta P_T d_f^\beta}$, $\varepsilon_f = \frac{(\alpha_f - \alpha_n \gamma_f) d_{p,f}^\beta}{\eta P_T d_f^\beta \gamma_f}$, and after some manipulations, we yields

$$P_{o,f}^1 = 1 - \Pr\left(|\hat{g}_{p,f}|^2 < \left(\varepsilon_f A_f^2 P_S - \tau_f\right), \varepsilon_f A_f^2 P_S > \tau_f\right)$$
$$\overset{(\kappa)}{=} 1 - \underbrace{\int_{\frac{\tau_f}{\varepsilon_f P_S}}^{\infty} F_{|\hat{g}_{p,f}|^2}\left(\varepsilon_f P_S y - \tau_f\right) f_Y(y) dy}_{I_1}. \qquad (A.6)$$

For step (κ), $\alpha_f > T_1$ is hold.

Denote $X_i = |\hat{g}_{p,i}|^2$, the corresponding PDF and CDF can be given by

$$f_{X_i}(x) = \frac{1}{\lambda_i} e^{-\frac{x}{\lambda_i}}, \qquad (A.7)$$

$$F_{X_i}(x) = 1 - e^{-\frac{x}{\lambda_i}}. \qquad (A.8)$$

where $\lambda_i = E\left(|\hat{g}_{p,i}|^2\right)$, $E(\cdot)$ denotes expectation operater.

As for $\alpha_f \leq T_1$, we can easily obtain $P_{o,f}^1 = 1$.

Substituting (A.2) and (A.8) into (A.6), we arrive at

$$I_1 =$$
$$\int_{\frac{\tau_f}{\varepsilon_f P_S}}^{\infty} \left(1 - e^{-\frac{\varepsilon_f P_S y - \tau_f}{\lambda_{p,f}}}\right) \frac{y^{\frac{a-1}{2}}}{2b^{a+1}\Gamma(a+1)} \exp\left(-\frac{\sqrt{y}}{b}\right) dy$$
$$= \underbrace{\int_{\frac{\tau_f}{\varepsilon_f P_S}}^{\infty} \frac{y^{\frac{a-1}{2}}}{2b^{a+1}\Gamma(a+1)} e^{-\frac{\sqrt{y}}{b}} dy}_{I_2} - \exp\left(\frac{\tau_f}{\lambda_{p,f}}\right)$$
$$\times \underbrace{\int_{\frac{\tau_f}{\varepsilon_f P_S}}^{\infty} \frac{y^{\frac{a-1}{2}}}{2b^{a+1}\Gamma(a+1)} \exp\left(-\left(\frac{\varepsilon_f P_S y}{\lambda_{n,f}} + \frac{\sqrt{y}}{b}\right)\right) dy}_{I_3}, \qquad (A.9)$$

where

$$I_2 = 1 - F_Y\left(\frac{\tau_f}{\varepsilon_f P_S}\right)$$
$$= 1 - \frac{\gamma\left(a+1, \frac{1}{b}\sqrt{\frac{\tau_f}{\varepsilon_f P_S}}\right)}{\Gamma(a+1)}. \qquad (A.10)$$

Let $t = \sqrt{y}$, I_3 in (A.9) can be written as

$$I_3 = \underbrace{\int_0^\infty \frac{t^a}{b^{a+1}\Gamma(a+1)} \exp\left(-\left(\frac{\varepsilon_f P_S}{\lambda_{p,f}} t^2 + \frac{t}{b}\right)\right) dt}_{I_4}$$
$$- \underbrace{\int_0^{\frac{\tau_f}{\varepsilon_f P_S}} \frac{y^{\frac{a-1}{2}}}{2b^{a+1}\Gamma(a+1)} \exp\left(-\left(\frac{\varepsilon_f P_S y}{\lambda_{p,f}} + \frac{\sqrt{y}}{b}\right)\right) dy}_{I_5}. \qquad (A.11)$$

Using $\int_0^\infty x^{v-1} e^{-\beta x^2 - \gamma x} = (2\beta)^{-\frac{v}{2}} \Gamma(v) \exp(\frac{\gamma^2}{8\beta}) D_{-v}\left(\frac{\gamma}{\sqrt{2\beta}}\right)$, I_4 can be given by

$$I_4 = \frac{1}{b^{a+1}} \left(\frac{2\varepsilon_f P_S}{\lambda_{p,f}}\right)^{-\frac{a+1}{2}} \exp\left(\frac{\lambda_{p,f}}{8b^2 \varepsilon_f P_S}\right)$$
$$\times D_{-(a+1)}\left(\frac{1}{b}\sqrt{\frac{\lambda_{p,f}}{2\varepsilon_f P_S}}\right). \qquad (A.12)$$

It isn't easy to get the exact closed-form of I_5. The Gauss-Chebyshev (GC) quadrature can be employed to obtain the approximate one, which can be written as

$$I_5 \approx \frac{\pi}{L} \sum_{l=1}^{L} \frac{\sqrt{1 - \phi_l^2}}{2b^{a+1}\Gamma(a+1)} \left(\frac{\tau_f}{2\varepsilon_f P_S}\right)^{\frac{a+1}{2}} (\phi_l + 1)^{\frac{a-1}{2}}$$
$$\times \exp\left(-\frac{\tau_f(\phi_l + 1)}{2\lambda_{p,f}} - \frac{1}{b}\sqrt{\frac{\tau_f(\phi_l + 1)}{2\varepsilon_f P_S}}\right). \qquad (A.13)$$

With the help of (A.6)-(A.13), the final expression of $P_{o,f}^1$ can be easily obtained by letting $i = f$ in (7). We introduce the general expressions for $\forall i$ to unify the results of $\mu = 1$.

APPENDIX B: PROOF OF THEOREM 2

In order to obtain the closed-form of (12), we should firstly get the results of $P_{o,n}^0$ and $P_{o,n}^1$ with $\mu = 0$ and $\mu = 1$ in (12). Letting $i = n$ and substituting (2) and (3) into $P_{o,n}^0$ in (12), we arrive at

$$P_{o,n}^0 = \Pr\left(A_n^2 > \frac{\psi_{1,n}}{P_S}, A_n^2 > \frac{\psi_{2,n}}{P_S}\right), \qquad (B.1)$$

When $\alpha_f \leq T_1$, we can easily obtain $P_{o,n}^0 = 0$; When $\alpha_f > T_1$, We arrive at

$$P_{o,n}^0 = \Pr\left(A_n^2 > \frac{\psi_n^*}{P_S}\right), \qquad (B.2)$$

Using (A.3), we arrive at

$$P_{o,n}^0 = 1 - \frac{\gamma\left(a+1, \frac{1}{b}\sqrt{\frac{\psi_n^*}{P_S}}\right)}{\Gamma(a+1)}, \qquad (B.3)$$

In another side, letting $i = n$ in (2) and substituting (2) and (3) into $P_{o,n}^1$ in (12) and letting $\mu = 1$, denotes $t_1 = \varepsilon_n A_n^2 P_S - \tau_n$, $t_2 = \varepsilon_{2,n} A_n^2 P_S - \tau_n$, we arrive at

$$P_{o,n}^1 \overset{(\kappa)}{=} \Pr\left(|\hat{g}_{p,n}|^2 < min(t_1, t_2), t_1 > 0, t_2 > 0\right). \qquad (B.4)$$

$$P_{o,f}^1 = \Pr\left(\frac{\alpha_f P_S A_f^2 d_f^{-\beta}}{\eta P_T\left(|\hat{g}_{p,f}|^2+\sigma_{e_{p,f}}^2\right)d_{p,f}^{-\beta}+\left(\alpha_n A_f^2+E_f\right)P_S d_f^{-\beta}+N_0} < \gamma_f\right), \qquad \text{(A.5)}$$

As to (B.4), when $\varepsilon_n \leq \varepsilon_{2,n}$, i.e. $\alpha_f \leq T_2$, $P_{o,n}^1$ can be given by

$$P_{o,n}^1 = \Pr\left(|\hat{g}_{p,n}|^2 < \varepsilon_n A_n^2 P_S - \tau_n, \varepsilon_n A_n^2 P_S > \tau_n\right)$$
$$= \int_{\frac{\tau_n}{\varepsilon_n P_S}}^{\infty} F_{|\hat{g}_{p,n}|^2}\left(\varepsilon_n P_S y - \tau_n\right) f_Y\left(y\right) dy.$$
$$\text{(B.5)}$$

Similar to the process for obtaining I_1 in (A.6), substituting ε_f and τ_f by ε_n and τ_n, we can easily obtain the results of (B.5).

When $\varepsilon_n > \varepsilon_{2,n}$, i.e. $\alpha_f > T_2$, $P_{o,n}^1$ can be given by:

$$P_{o,n}^1 = \Pr\left(|\hat{g}_{p,n}|^2 < \varepsilon_{2,n} A_n^2 P_S - \tau_n, \varepsilon_{2,n} A_n^2 P_S > \tau_n\right)$$
$$= \int_{\frac{\tau_n}{\varepsilon_{2,n} P_S}}^{\infty} F_{|\hat{g}_{p,n}|^2}\left(\varepsilon_{2,n} P_S y - \tau_n\right) f_Y\left(y\right) dy.$$
$$\text{(B.6)}$$

Similar to the results of (B.5), substituting ε_f and τ_f by $\varepsilon_{2,n}$ and τ_n, we can easily obtain the results of (B.6).

When $\alpha_f \leq T_1$, we can easily obtain $P_{o,n}^1 = 1$.

ACKNOWLEDGEMENT

REFERENCES

[1] D. -T. Do, T. Anh Le, T. N. Nguyen, X. Li and K. M. Rabie, "Joint Impacts of Imperfect CSI and Imperfect SIC in Cognitive Radio-Assisted NOMA-V2X Communications," *IEEE Access*, vol. 8, pp. 128629-128645, 2020.

[2] M. Li, X. Yang, F. Khan, M. A. Jan, W. Chen and Z. Han, "Improving Physical Layer Security in Vehicles and Pedestrians Networks With Ambient Backscatter Communication," *IEEE Transactions on Intelligent Transportation Systems*, vol. 23, no. 7, pp. 9380-9390, July 2022.

[3] H. Ding, C. Zhang, Y. Cai and Y. Fang, "Smart Cities on Wheels: A Newly Emerging Vehicular Cognitive Capability Harvesting Network for Data Transportation," *IEEE Wireless Communications*, vol. 25, no. 2, pp. 160-169, April 2018.

[4] B. Di, L. Song, Y. Li and Z. Han, "V2X Meets NOMA: Non-Orthogonal Multiple Access for 5G-Enabled Vehicular Networks," *IEEE Wireless Communications*, vol. 24, no. 6, pp. 14-21, Dec. 2017.

[5] M. Li, H. Yuan, C. Maple, W. Cheng and G. Epiphaniou, "Physical Layer Security Analysis of Cognitive NOMA Internet of Things Networks," in IEEE Systems Journal, vol. 17, no. 1, pp. 1045-1055, March 2023.

[6] M. Noor-A-Rahim et al., "6G for Vehicle-to-Everything (V2X) Communications: Enabling Technologies, Challenges, and Opportunities," *Proceedings of the IEEE*, vol. 110, no. 6, pp. 712-734, Jun. 2022.

[7] S. Arzykulov, T. A. Tsiftsis, G. Nauryzbayev and M. Abdallah, "Outage Performance of Cooperative Underlay CR-NOMA With Imperfect CSI," *IEEE Communications Letters*, vol. 23, no. 1, pp. 176-179, Jan. 2019.

[8] Le, CB., Do, DT., Zaharis, Z.D. et al., "System Performance Analysis in Cognitive Radio-Aided NOMA Network: An Application to Vehicle-to-Everything Communications," *Wireless Pers Commun 120*, vol. no, pp. 1975–2000, 2021.

[9] C. Song, H. Zhang, Y. Li, H. Zhang, E. Li, and K. Hu, "Outage Performance Analysis of CR-NOMA Based on Incremental Relay," *Wireless Communications and Mobile Computing*, vol. no, pp. 1-26, 2022.

[10] A. Hemanth, K. Umamaheswari, A. C. Pogaku, D. -T. Do and B. M. Lee, "Outage Performance Analysis of Reconfigurable Intelligent Surfaces-Aided NOMA Under Presence of Hardware Impairment," *IEEE Access*, vol. 8, pp. 212156-212165, 2020.

[11] M. Li, H. Yuan, C. Maple, Y. Li and O. Alluhaibi, "Security Outage Probability Analysis of Cognitive Networks With Multiple Eavesdroppers for Industrial Internet of Things," *IEEE Transactions on Cognitive Communications and Networking*, vol. 8, no. 3, pp. 1422-1433, Sept. 2022.

[12] Q. Chen, M. Li, X. Yang, R. Alturki, M. D. Alshehri and F. Khan, "Impact of Residual Hardware Impairment on the IoT Secrecy Performance of RIS-Assisted NOMA Networks," in IEEE Access, vol. 9, pp. 42583-42592, 2021.

[13] Y. Ai, F. A. P. deFigueiredo, L. Kong, M. Cheffena, S. Chatzinotas and B. Ottersten, "Secure Vehicular Communications Through Reconfigurable Intelligent Surfaces," *IEEE Transactions on Vehicular Technology*, vol. 70, no. 7, pp. 7272-7276, Jul. 2021.

[14] V. K. S. Primak and V. Lyandres, "Stochastic Methods and their Applications to Communications: Stochastic Differential Equations Approach", *Stochastic Methods and Their Applications to Communications*, vol. no, pp. Jul. 2004.